

# FEM RESEARCHES REGARDING INCREMENTAL FORMING PROCESS

Ionut CHERA<sup>1</sup>, Octavian BOLOGA<sup>2</sup>, Gabriel RACZ<sup>3</sup>, Radu BREAZ<sup>4</sup> and Mihai CRENGANIS<sup>5</sup>

<sup>1</sup>"Lucian Blaga" University of Sibiu, Romania, Faculty of Engineering, ionut.chera@ulbsibiu.ro  
<sup>2</sup>"Lucian Blaga" University of Sibiu, Romania, Faculty of Engineering, octavian.bologa@ulbsibiu.ro  
<sup>3</sup>"Lucian Blaga" University of Sibiu, Romania, Faculty of Engineering, gabriel.racz@ulbsibiu.ro  
<sup>4</sup>"Lucian Blaga" University of Sibiu, Romania, Faculty of Engineering, radu.breaz@ulbsibiu.ro  
<sup>5</sup>"Lucian Blaga" University of Sibiu, Romania, Faculty of Engineering, mihai.crenganis@ulbsibiu.ro

**Abstract**— Incremental sheet metal forming is a relatively new forming process that can provide a cheap way to manufacture sheet metal parts without the need of expensive dies. The goal of this research is to determine if an asymmetric incremental sheet metal forming process can be executed by means of a KUKA industrial robot. The most important aspects that have been taken into account regarding the incremental forming process done by means of an industrial robot were the forces variation, thickness reduction and the major principle strain variation. The first step in order to determine these factors was to obtain the stress-strain curve for the steel sheet used for the experimental parts. Once the stress-strain curve is obtained, a numerical simulation of the incremental sheet metal process can be performed by means of LS-Dyna software.

**Keywords**— finite element method, incremental sheet metal forming, industrial robot, strains

## I. INTRODUCTION

IN recent years the market demanded a new approach to sheet metal processes as traditional techniques cannot keep up with the rapid changes within the industrial manufacturing environment. Technology makes increasingly more progresses and new flexible solutions emerge, lowering production costs and time. Incremental forming is such a process, best suited for producing low cost prototypes and pre-series components [1], [2]. Unlike traditional metal forming processes, performing fast production changes are possible due to the simplistic machine configuration. Although the time required to manufacture a product is longer than on a traditional forming press, the time spent on tool design and prototype production is significantly shorter.

Incremental forming of sheet metal parts can be performed on a diverse set of machines like specially constructed incremental forming machines, CNC milling machines and more recently by means of industrial robots [3], [4].

Incremental sheet metal forming caught the interest of scientific research groups very early on because of its great potential and applicability in various fields. Promising results were reported in manufacturing medical implants by means of single point incremental forming [5].

## II. INCREMENTAL FORMING

A brief description of the SPIF process principle is presented in Fig. 1. The blank (2) is fixed by means of the blank holder (3). In order to shape the sheet metal part, the punch (1) has an axial feed movement on vertical direction, continuous or in steps  $s$  (incremental), while the other element, the active plate (4) carries out a plane horizontal movement.

Incremental forming enables a higher degree of deformation and the possibility of forming materials with reduced deformation capacity and higher strength [6].

In spite of its great advantages, the industry is still reluctant to apply incremental forming on a large scale due to two major drawbacks: low shape and dimensional accuracy of the sheet metal parts and sheet metal integrity [7]. Some solutions have been identified in order to eliminate these drawbacks; one of the most promising is the optimization of the process tool paths [8].

A large number of research results about incremental forming have been published in recent years, aiming to find out what machine is best suited for this process and of course what are the most important process parameters both in running experiments and for production [9].

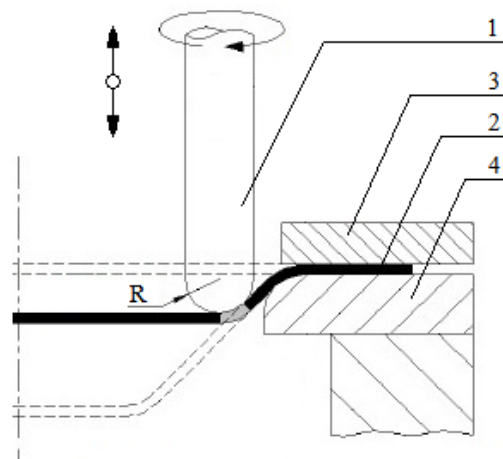


Fig. 1. Process principle of single point incremental forming

Although in the first articles regarding this process experiments were done with the help of special machines or CNC milling machines, in recent years a large number of articles were published in which the authors have conducted experiments using industrial robots [6], [10].

### III. ROBOTIC SYSTEM USED FOR INCREMENTAL FORMING

The experimental layout used for the incremental forming consists of a six degrees of freedom anthropomorphic robot KUKA KR 6 Fig. 2, a custom blank holder, a custom tool holding unit and the forming tool. The KUKA KR6 robot has great flexibility and is suitable for both point-to-point and continuous-path controlled tasks [11].

The position and the orientation of the blank holder were chosen in this manner, so that an optical measuring system like ARAMIS can be used in order to measure the strains during the incremental forming process.

The goal of this research is to determine if an asymmetric incremental sheet metal forming process can be performed by means of this KUKA KR 6 industrial robot.

### IV. IDENTIFICATION OF THE SHEET METAL MATERIAL PROPERTIES

In order to test the deformability of a material, the most utilized method is the uniaxial tensile test. The test specimen is fixed on both sides inside a tensile testing machine, and deformed at a constant speed until the breaking point. The force applied on the test specimen is measured by a force transducer and the strain with an extensometer. The obtained data can be graphically represented directly in load-displacement coordinates. However, they are generally converted into the stress-strain coordinates. In addition, for determining the deformability of the material, a common practice is to measure the width of the specimen during the actual test.



Fig. 2. Experimental layout for incremental forming



Fig. 3. Experimental layout for tensile test

The width is measured either intermittently by interrupting the test, either continuously by means of an extensometer.

The determination of the material properties was done using the Instron 5587 tensile testing machine Fig. 3 following the steps:

- a St 14 steel sheet with the thickness of 0.4 mm was chosen for the tensile test;
- a series of five samples for each orientation of specimen were cut from the original sheet metal;

Because the properties of the material can vary depending on the considered direction relatively to the rolling direction of the sheet, the anisotropy of the material can also vary. Taking this fact into account, the samples were first cut in the longitudinal direction, parallel to the rolling direction of the sheet, then perpendicular to the rolling direction of the sheet, and finally at a 45° angle relatively to the rolling direction of the sheet. The shape and dimensions of the specimens were taken according to SR EN 10002-1/1995.

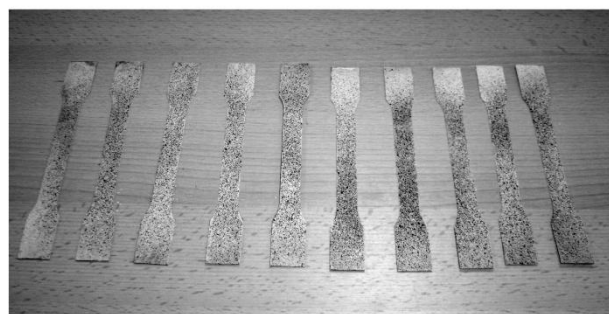


Fig. 4. Prepared specimens

- a test method was developed using the software provided with the tensile test machine; in this stage the following were determined : the specimen's shape, thickness of the material, the width of the specimen, the distance between the jaws of the machine, the distance between measuring references, the speed of traction, the limitation points for the machines, the rate of acquisition of the machine (200 dots/second), the output file type (ASCII or DIF – Data Interchange Format, a file that can be visualized and processed by any statistical data processing programs), the type of output data to be collected;
- the output data are : the elastic modulus (MPa), the maximum stress in the material (MPa), the relative elongation of the material at the maximum stress in the material (%), K- strength coefficient (MPa), n- strain hardening exponent.
- in addition to the information mentioned above, Aramis system is used as an extensometer in order to measure the strains. Aramis uses a diffuse network of points applied on the surface of the test pieces, Fig. 4, and is able to measure the displacements between these points during the deformation process and thus it can determine the principle strains.

The curves of true equivalent stress-true plastic strain obtained from the tensile test, for a specimen at the direction parallel to the rolling direction of the sheet are presented in Fig. 5.

The stress of the plastic flow for a classical hardening exponential law is defined by the following Swift relation:

$$\sigma_y = K_y(\epsilon_0 + \epsilon)^n \quad (1)$$

where  $K_y$  is the strength coefficient,  $\epsilon_0$  is appropriate initial elongation corresponding to limit of elasticity,  $\epsilon$  is the corresponding plastic strain and  $n$  is the hardening coefficient.

Concerning the  $\epsilon_0$  value, it can be computed from the Yield tensile stress  $\sigma_{00}$  using the formula:

$$\epsilon_0 = \left(\frac{\sigma_{00}}{K_y}\right)^{1/n} \quad (2)$$

All the material parameters were computed from the Bluehill software and are presented in the Table I.

After calculating the anisotropic coefficients the following results were obtained :  $R_{00} = 0,99$ ;  $R_{45} = 0,936$ ;  $R_{90} = 1.12$ ,  $\bar{R} = 0.997$ .

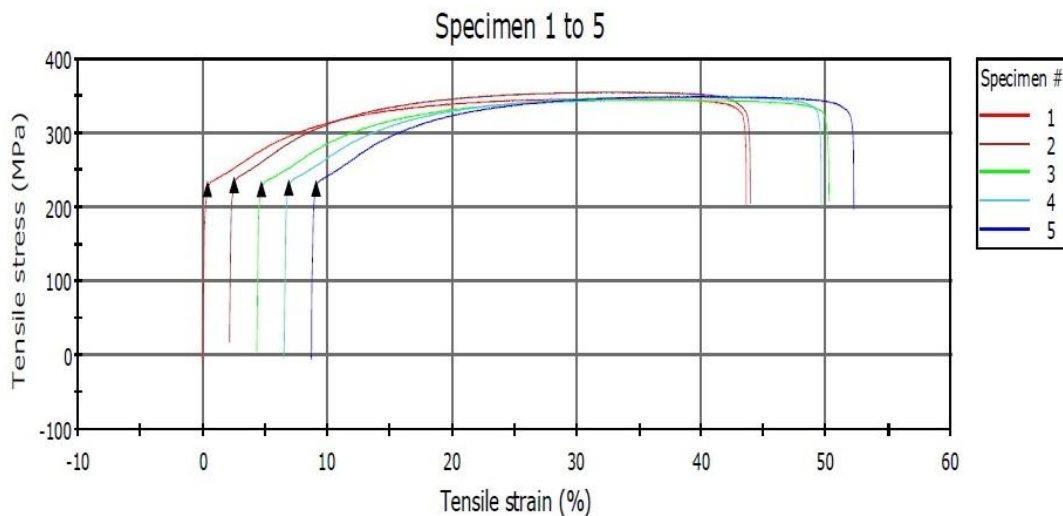


Fig. 5. The stress-strain curve for St 14 steel sheet

TABLE I THE MATERIAL CHARACTERISTICS OBTAINED BY UNIAXIAL TENSION TEST FOR ST 14 STEEL SHEET

Specimen no.	E - Young modulus	Yield Tensile stress	Maximum Tensile stress	Tensile strain at Maximum Tensile stress	n - Strain Hardening Exponent	$K_y$ - Strength Coefficient
	(MPa)	(MPa)	(MPa)	(%)	-	(MPa)
1.	70016	224.77	346.46	43.57	0,231	603.42
2.	70016	230.52	355.32	41.71	0,219	606.03
3.	70016	224.47	344.72	45.84	0,214	582.29
4.	79278	226.48	348.78	43.03	0,212	587.35
5.	80302	225.57	349.35	43.45	0,213	588.72
Average	73925.6	226.362	348.926	43.52	0,217	593.562



## V. NUMERICAL SIMULATION

In order to resolve the non-linear analysis, a parameterized model of the incremental formed part was built by means of LS-Dyna software Fig. 8. This model was then used in the finite element analysis described through the LS-Dyna software.

The forming system that is being used as base for the numerical simulations consists of a die, blank holder and hemispherical punch. The blank consists of a square sheet (250mm x 250mm), which is placed on an active die with a square shaped working zone.

The dimensions of the opening of the active die are 200mm x 200mm. There are not imposed boundary conditions on the nodes placed on the edge of the active edges because the blank holder eliminates this necessity.

The shape of the incremental forming part is a truncated pyramid and is presented in Fig. 6. The trajectory used for the finite element simulations is presented in Fig. 7.

The punch follows a series of square shaped trajectories in order to create the truncated pyramid shape part. Between each square the punch advances in the Z direction in small increments, the step size is 0.1 mm.

In order to simulate the surface of the part, the LS-Dyna material model 37 (Transversely Anisotropic Elastic-Plastic) was chosen because it can accommodate in-plane and isotropic yield behavior.

The average values obtained by experimental identification were used in the finite element simulation.

The elasticity modulus is  $E = 123.538$  GPa, Poisson's coefficient is  $\nu = 0.3$ , density  $\rho = 7.85e^{-9}$  tons/mm<sup>3</sup> while the flow stress is  $\sigma_y = 227.218$  MPa, strength coefficient  $K = 593.562$  MPa and hardening coefficient  $n = 0.217$ .

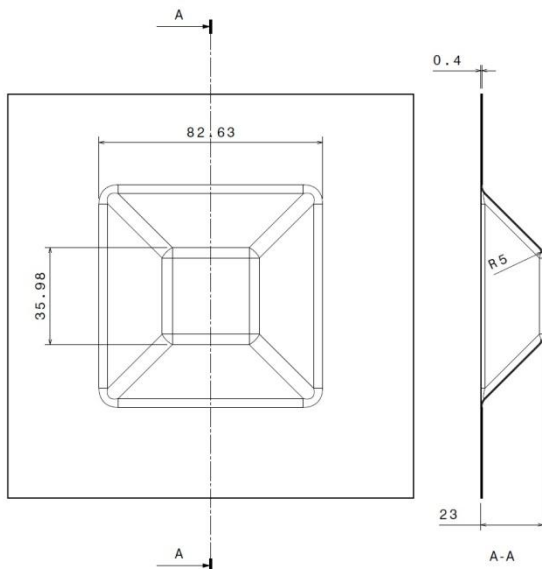


Fig. 6. Dimensions of the test part

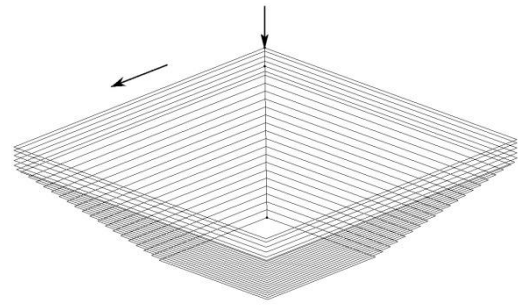


Fig. 7. Trajectory used in the finite element analysis

The finite element network associated with the part's geometry is built in such a way that it allows an unfolding of the analysis in good conditions, without requiring a re-discretization because of its exaggerated distortions.

The part, discretized as a shell and a deformable body, is composed of 2441 Thin-Shell-163-type elements. Because of the way in which the elements are connected, the network contains 9838 nodes.

A shear factor of 5/6 and a total of 11 integration points through the thickness were used in order to record the variation of the stresses and strains through the thickness of the material. The hourglass control based on Belytschko and Tsay viscous formulation was selected in order to avoid problems with single point Gaussian integration. The value for the friction coefficient that was used is 0.08.

This kind of plastic deformation process is difficult to control, due to some characteristic aspects such as: a relatively small contact surface of the tools with the blank; the strains appearing in the material must be superior to those which bring it in the plastic state, but they must be less than the critical ones; the state of biaxial stretching is the least favourable to the plastic deformation processes. Because of this fact, the results of the numeric analyses in the non-linear field are oriented towards the description in a qualitative and quantitative way of the strain process results.

For the finite element analysis, a sphere with the diameter of 10 mm was used to simulate the punch. The material thickness of the sheet was 0.4 mm.

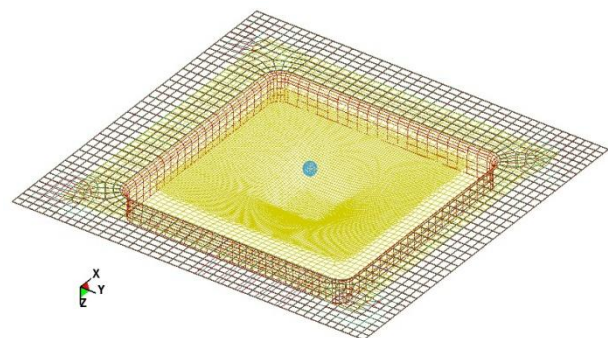


Fig. 8. Parameterized model for the incremental formed part

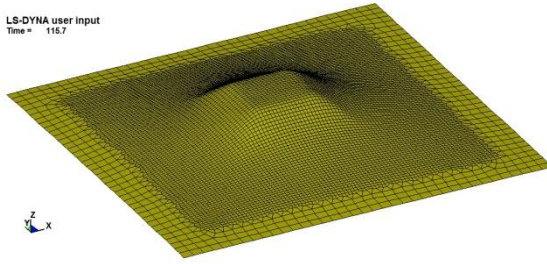


Fig. 9. Final shape of the test part resulted from the finite element analysis

The intention of the authors was to simply verify if the actual incremental forming process could be performed for the given St 14 sheets by means of the KUKA KR6 industrial robot.

The shape of the test part resulted from the finite element analysis is presented in Fig. 9.

The numerical results of the simulations were focused on the determination the thinning variation, the major strains and the forces of the incremental forming process. For major and minor strains we chose the engineering (technical) strains in order to compare the results with future experimental ones.

As the results from the finite element analysis are analyzed, it can be concluded that the maximum values of the major strain Fig. 10 and those of the minor strain Fig. 11 are in within acceptable limits.

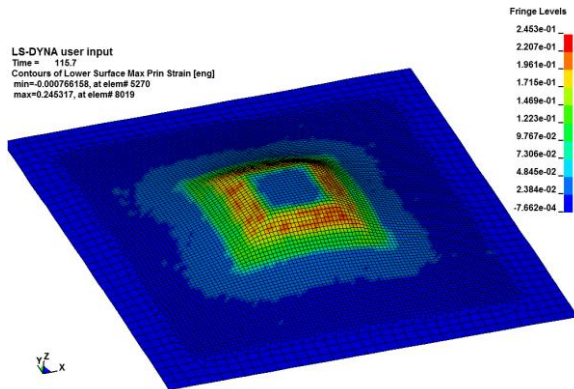


Fig. 10. The major principle strain variation

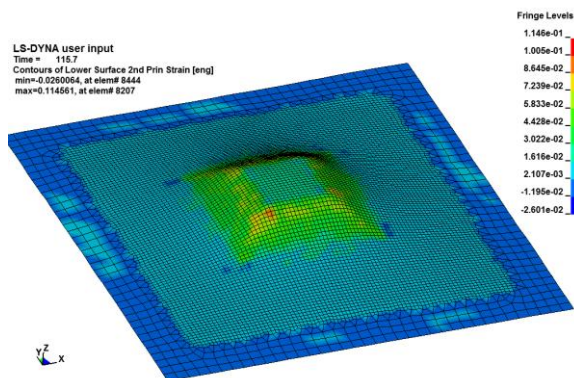


Fig. 11. The minor principle strain variation

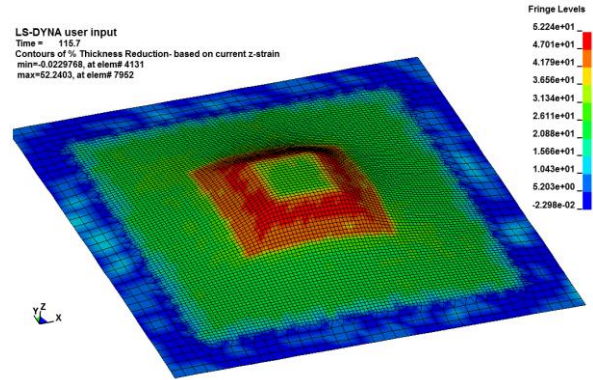


Fig. 12. The thinning variation resulted from the finite element analysis

The maximum value of 0.245 for the major strains was attained on the faces of the truncated pyramid shaped part. The maximum value of 0.114 for the minor strains was attained on the corners of the truncated pyramid shaped part.

The results regarding the thinning variation (52.24%) that was obtained from the finite element analysis are presented in Fig. 12.

The maximum value of the  $F_x$  component is 59.44 N. The variation of the force on the  $F_x$  component is presented in Fig. 13. The maximum value of the  $F_y$  component is 73.04 N, Fig. 14 and for the  $F_z$  component is 228.11 N, Fig. 15.

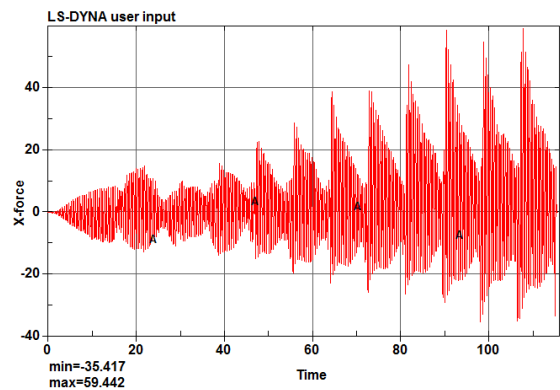


Fig. 13. Force variation for the  $F_x$  component

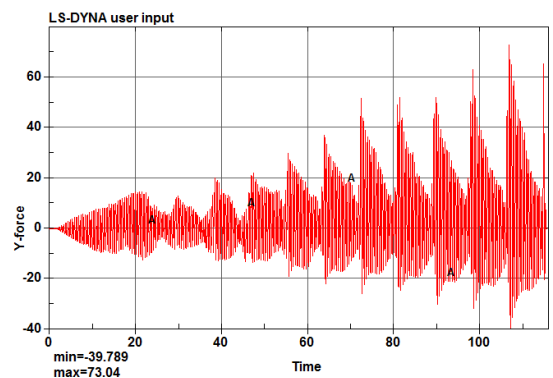


Fig. 14. Force variation for the  $F_y$  component

